EXPERIMENTAL ASSESSMENT OF SUSPENDED SEDIMENT CONCENTRATION CHANGED BY SOLITARY WAVE

Jae-Nam Cho
Department of Civil Engineering, Hongik University, 94 Wausan-ro, Mapo-gu, Seoul, Republic of Korea.

Chang-Geun Song
Department of Safety Engineering, Incheon National University, Incheon, Republic of Korea.

Kyu-Nam Hwang
Department of Civil Engineering, Chonbuk National University, 567 BaekjeDaero, Deokjin-gu Jeonju-si, Jeollabuk-do, Republic of Korea.

Seung-Oh Lee
Department of Civil Engineering, Hongik University, 94 Wausan-ro, Mapo-gu, Seoul, Republic of Korea.,
seungoh.lee@hongik.ac.kr

Follow this and additional works at: https://jmstt.ntou.edu.tw/journal

Part of the Engineering Commons

EXPERIMENTAL ASSESSMENT OF SUSPENDED SEDIMENT CONCENTRATION CHANGED BY SOLITARY WAVE

Acknowledgements

EXPERIMENTAL ASSESSMENT OF SUSPENDED SEDIMENT CONCENTRATION CHANGED BY SOLITARY WAVE

Jae-Nam Cho[1], Chang-Geun Song[2], Kyu-Nam Hwang[3], and Seung-Oh Lee[1]

ABSTRACT

A large scale solitary wave causes a lot of sediment transportation and coastal beach erosion, for example tsunami is the one type of solitary waves. During passing such solitary wave over coastal region, higher energy on sediment transportation near bottom would bring to massive geomorphological changes and even worse damages in life and economics. The major objective of this study is to analyze the incipient motion of sediment suspended from bottom by a solitary wave through hydraulic experiments and numerical simulations. First, to estimate the process of sediment transport the experimental study was carried out in the prismatic rectangular channel of 12 m in length, 0.8 m in width and 0.75 m in height. Solitary waves were generated by an abrupt opening of a sluice gate upstream for several water depth conditions. Two different types of sediments were used: Joomoonjin sand (d_{50} = 0.58 mm, SG = 2.65) and anthracite (d_{50} = 1.55 mm, SG = 1.61). Before starting each experiment, sediments were laid out with the thickness of 0.3 m on the slope of 1/6. During each experiment, turbidities were measured by sampling suspended sediment concentrations at 5 collecting points, which were used to calibrate the numerical simulations. Numerical simulations using the FLOW-3D with the GMO (General Moving Object) module were performed to investigate the relationship between turbulence intensity and suspended sediment concentration (SSC) after the validation with experiment results. It was found that SSC was mainly affected by the wave height and run-up/down velocity along a slope for a solitary wave passage. Turbulence intensity was considered as the most effective factor to comprehend the overall pattern of SSC distributions when turbulence of solitary wave was analyzed through the regression analysis. Finally, each non-dimensional empirical formula was suggested to estimate SSC occurred by a solitary wave passage for plunging and spilling break types, respectively. Moreover, results from this study would provide fundamental assessment to bridge between solitary wave characteristics and SSC based on laboratory experiments and numerical simulations.

I. INTRODUCTION

Solitary waves would cause serious damages to human being, coastal structures and environmental process, especially in shorelines. They would also induce severe amount of suspended sediment transportation over a widely broad area in coastal regions because they are commonly considered as long period waves, which can occur impulsive geophysical changes on coastal areas. Especially, run-up and run-down during a solitary wave passage along beach slope can accompany with grave coastal sediment erosions. Most field observations, however, showed that it is relatively hard to measure the related parameters such as the erosion rate and to describe the morphological dynamics of coastal lines when solitary wave approaches to shallow water regions and shorelines (Munk, 1949). Erosion and deposition occurred during the process of solitary wave propagation have rarely been known about the methodology to evaluate or estimate suspended sediment, particularly at run-up and run-down. Thus, it is necessary to analyze the relationship between solitary waves and erosion phenomenon when rapid bed changes are occurred because of the solitary wave that transports coastal sediments to shorelines.

Turbulence generated by wave breaking should variously affect sediment transport, especially re-suspension for different breaking types. In the literature, laboratory experiment results have indicated the relation between the importance of initial wave profiles for swash zone and the sediment capacity of a single solitary wave (Kobayashi and Lawrence, 2004). Effects of approaching solitary waves on a sandy beach were analyzed for various slopes to probe sediment transport and morphological

changes (Moronkeji and Rolla, 2007). Bed transport amounts and profiles were examined under the single solitary wave alone. Most experimental researches on the erosion and deposition mechanism occurred by solitary waves showed that velocity in similar behavior and shear stress were less relatively affected (Tsujimoto et al., 2008). In those studies, the tendency of the erosion and deposition in coastal areas have been simply investigated and they have proved that the run up and run down of solitary waves could induce considerable sediment transports of fine sand slope because of excess pressure differences. When many researchers have studied sediment transport mechanisms caused by a solitary wave, they have conducted experiments near the location of breaking wave point on a slope. Turbulent energy dissipation of a solitary wave was associated with a breaking type and was ranged from 20 to 60% (Chanson and Maruyama, 2002). Influence of surface waves on onshore stream was much considered rather than grain sizes of sediments (Dohmen and Janssen, 2001). Energy dissipation at solitary wave breaking was investigated with only numerical simulations (Arthur and Fringer, 2014). Nevertheless, the study about the quantitative analysis of suspended sediment caused by a solitary wave is still needed at the scientific investigations and field applications. Also, it is necessary to research with laboratory experiments for solitary waves on the turbulence characteristics which would disturb the sediments near the bottom on a slope. Most previous studies have not presented the quantitative analysis to suspended sediment concentration on a slope using the turbulence mechanism.

In this study, the experimental investigations and numerical simulations were conducted to understand the sediment transport near the bottom along a slope when the passage of solitary waves which were induced by the abrupt change of water level between upstream and downstream of a sluice gate with the controlled opening speed. Also, a turbulence intensity near the bottom and run up/down velocities on a slope were investigated during a solitary wave passage with the conjunction of experimental and numerical results.

Experimental results are investigated how much suspended sediment concentration (SSC) was affected by the run up and run down along a slope during a solitary wave passage. From overall combined results from experiments and numerical simulations, new information provides prominence about the breaking wave type and run up/down velocities on a slope in solitary wave for the sediment transport formulae about SSC.

II. EXPERIMENTAL SETUP

Based on the Boussinesq approximation, the linear shallow-water wave height was small compared to water depth and depth averaged velocity which are presented as following as Eqs. (1) and (2) (Carrier and Greenspan, 1958; Synolakis, 1987).

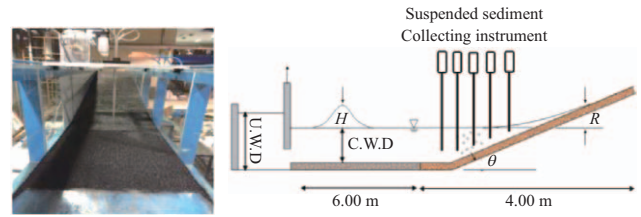$$\eta = H sech^2 \sqrt{\frac{3H}{4h^3}}(x - ct) \tag{1}$$

Fig. 1. Experimental open channel and schematic diagram.

Fig. 2. Solitary wave propagation in experiment and ASC (Absorptive SSC Collector).

$$u = \eta \sqrt{\frac{g}{h}} \tag{2}$$

where, H is the solitary wave height (m), h is the channel water depth (m), c is the solitary wave celerity ($= \sqrt{g(H+h)}$), η is the solitary wave amplitude (m) and u is the depth average velocity.

As shown in Fig. 1, the prismatic open channel was used with the length of 12.0 m, the width of 0.8 m and the height of 0.75 m. At the end of channel, a slope of 1/6 was constructed with acrylic plates. Also, one side wall of the experimental channel has become transparent to observe the propagation of a solitary wave ($2.0 < x < 12.0$ m in x-direction) which generated from upstream. And the side view motions of breaking wave were kept a close watch to identify the breaking types, such as plunging and spilling. Solitary wave shape and run up/down velocity were measured by two video cameras with the frequency of 30 Hz (SONY, HDR-XR550) to estimate the velocity for run up/down on a slope.

Table 1. Experimental conditions and solitary wave characteristics.

	Case	U.W.D.(m) Upstream Water Depth	C.W.D (m) Channel Water Depth	Solitary wave characteristics			
				H (m)	L (m)	C (m/s)	T (s)
1	AC/JS 30.0-20.0	0.300	0.200	0.022	3.033	1.59	0.549
2	AC/JS 32.5-20.0	0.325	0.200	0.026	2.771	1.83	0.602
3	AC/JS 35.0-20.0	0.350	0.200	0.031	2.597	2.07	0.671
4	AC/JS 35.0-25.0	0.350	0.250	0.023	4.134	1.64	0.438
5	AC/JS 37.5-25.0	0.375	0.250	0.029	3.641	1.94	0.526
6	AC/JS 40.0-25.0	0.400	0.250	0.037	3.286	2.10	0.652
7	AC/JS 42.5-25.0	0.425	0.250	0.045	3.004	2.26	0.739
8	AC/JS 45.0-25.0	0.450	0.250	0.053	2.726	2.44	0.846

AC: anthracite, JS: Joomonjin sand
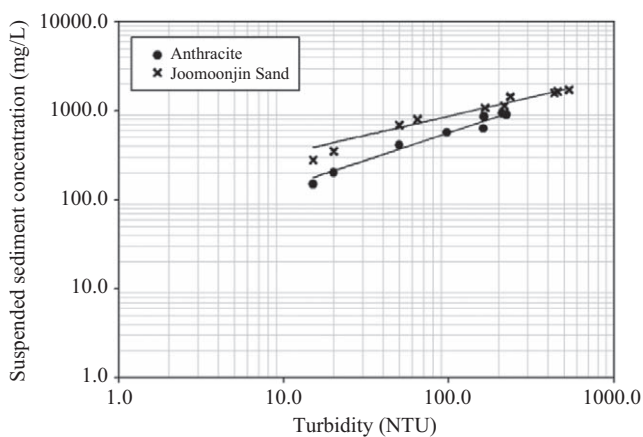
Fig. 3. Relation curve between suspended sediment concentration versus turbidity.

After a sluice gate abruptly opening, wave characteristics like solitary wave height, celerity and shape were decided as shown in Fig. 2. When it approached to a slope, it invoked suspended sediment concentration (SSC), turbidity and wave breaking on a slope.

In each experiment, the solitary wave propagation and sediment turbidity were video recorded from the time of the opening the sluice gate to the point that the wave reflected at the sluice gate. At the same time, suspended sediment during the wave passing was collected by the in-house manufactured SSC equipment as shown in Fig. 2. The SSC system was designed to capture suspended sediment concentrations at five specific points during solitary wave run up and run down on a slope. Also, it is possible to make use of the equipment in the coastal field for fine sandy slope. After solitary wave passing, at least 25 ml of the suspended sediment samples were absorbed during 0.54 - 0.92 secs by the SSC system. Also, each turbidity of suspended sediments simultaneously was measured to verify suspended sediment concentration with the turbidity meter (Model: TN-100, Eutech). The relationship between SSC and turbidity iss presented in Fig. 3, with $R^2 = 0.945$ for Joomonjin sand and $R^2 = 0.983$ for anthracite, respectively. Initial conditions and parameters of the experiments are presented in Table 1.

Regression analysis shows a linear relationship between SSC and turbidity, given that the sediment concentration is as equally scattered as the amount of light evident when measuring turbidity (Pavanelli and Pagliarani, 2002). Even though the spatial measurement of SSC should be sophisticated compared to sediment turbidity, it could be presented the reliable results from the relationship between SSC and turbidity established in Fig. 3. In this study, this relationship was used to provide spatial SSC distribution, especially near the bottom along a slope after image processing to reveal the spatial distribution of sediment turbidities from each experimental result.

As described above, a sluice gate at upstream end of the open channel was used to generate specific solitary waves by being rapidly opened, thereby exposing a difference in water depths between upstream and downstream positions that resulted in wave formation.

For a channel water depth (C.W.D) of 0.200 - 0.250 m and upstream water depth (U.W.D) of 0.300 - 0.450 m, a solitary wave height (H) of 0.022 - 0.053 m, and wave period (T) of 0.512 - 0.785 s were measured. A movable sediment layer 0.3 thick was built by spreading sediment out along a slope of 1:6 gradient slope at the beginning of each experiment. Anthracite and Joomoonjin sand, have mean sediment diameter (d50) of 0.58 mm and 1.55 mm, specific gravity (SG) of 1.61 and 2.65 and coefficient of uniformity of 1.68 and 1.18, respectively. The particle size distributions of two sediments are shown in Fig. 4.

III. NUMERICAL SIMULATIONS

Numerical simulations were performed under same as experiments using the FLOW-3D (Flow science Inc., 2010). Solitary waves were produced with the GMO (General Moving Object) module in the software by prescribing the motion of sluice gate. The renormalized group simulation model (RNG) was employed for turbulence closure from directly computing all turbulence occurred during a solitary wave passage. The size of the computational grid and approximate features were too small to be resolved, resulting in the effect of turbulence being represented by the eddy viscosity in the RNG model, which is proportional
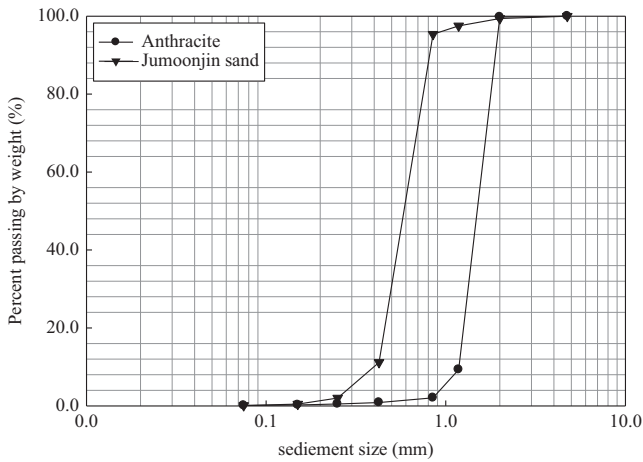
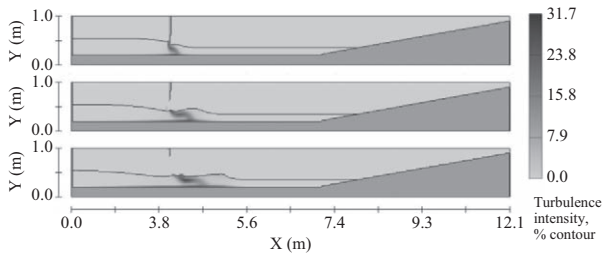**Fig. 4. Particle size distribution of experimental sediments.**

Fig. 5. Numerical simulation by FLOW-3D with GMO.

Fig. 6.   Verification between experiment and numerical simulation results.

to a length scale multiplied by a measure of velocity fluctuation. (Smagorinsky, 1991).

Although this model can overestimate undertows at the inner bore, it was adopted in most cases related to solitary waves. In practice, it showed relatively accurate prediction simulation results for solitary wave crest distribution in wave plunging and spilling breaking case (Zhao and Tanimoto, 2004). To generate the same solitary waves as in the hydraulic experiments, 1,440,000 grids were used in each simulation. Each grid has the dimension of $\Delta x \times \Delta y \times 1 \text{ cm} \times 1 \text{ cm} \times 1 \text{ cm}$. The averaged depth velocity, wave height and turbulence intensity of each solitary wave were obtained from each numerical result to examine characteristics of sediment transport phenomenon near the bottom. An example of the propagation of a solitary wave that displays similarities between experiment and numerical simulation is shown in Fig. 5. Wave height, velocity and celerity values also showed a good agreement with experimental results (Fig. 6). Hence, numerical method provides reliable calculation of hydrodynamic conditions during solitary wave motion. It is also found from numerical results sediment transport during solitary wave propagation is most affected by turbulence intensity, which is related to the wave breaking on a slope.

Numerical simulations also proved accurate for both solitary wave propagation and breaking waves during run up and run down over a slope. For all cases, both temporal and spatial errors were examined to ensure they were < 5.0% during solitary wave propagation in both experimental and numerical results.
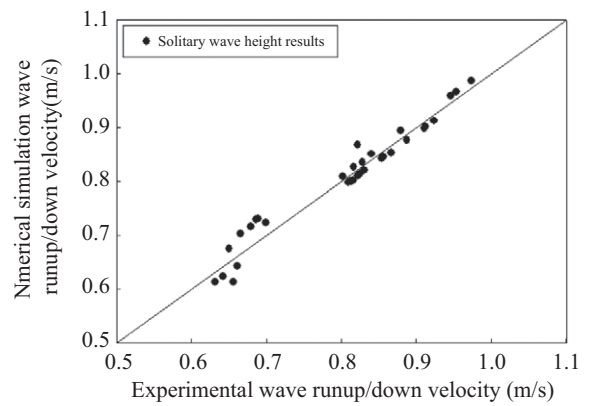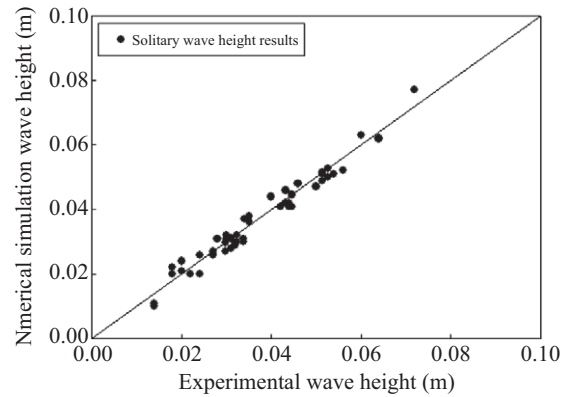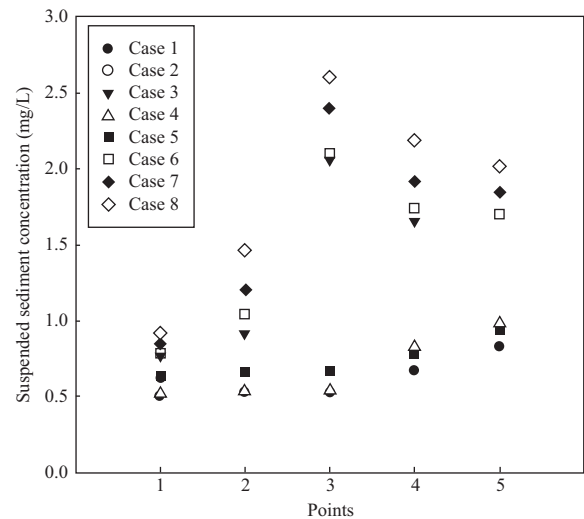

Fig. 7. Experimental results of suspended sediment concentration.

IV. RESULTS

Each experiment was conducted to measure the occurrence of SSC during a solitary wave passage. Particularly, the measurement of SSC was carried out for the time when run up/down occurred on the slope. Five collection points were used to measure SSC, as shown in Fig. 7. The results show that the SSC became
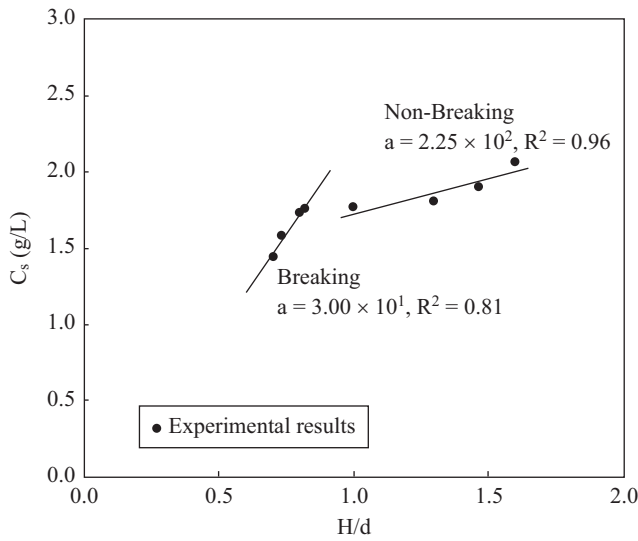
Fig. 8. Suspended sediment concentration curve against H/d.

Fig. 9. Turbulence intensity curve against H/d.

highest at Point 3 became it is closest to the breaking point of the wave, and thus is subject to high-energy transport of sediment related to the strong turbulence intensity in the hydrodynamic regime.

In terms of wave breaking type, it was found that there are two clear sections that can be classified. The first section is referred to as the spilling breaking type, which occurred when the difference of water depth between U.W.D and C.W.D was in the 0.100 - 0.150 m range. The second is referred to as the plunging breaking type, which occurred when the difference of water depth between U.W.D and C.W.D was in the 0.175 - 0.250 m range. Because the difference of water depths between U.W.D and C.W.D. could have different potential energy which would convert to form a solitary wave. Hence, the much potential energy induced by a sluice gate, the higher solitary wave heights. Indeed, the breaking point of each solitary wave shows highly disturbed bed sediment. Simple calculations show that Point 3 was approximately equal to the breaking points in most cases, indicating that the highest SSC value along the slope occurred at Point 3.

Results from Fig. 8 show how much SSC is strongly dependent on solitary wave height. To examine this relationship, the relative wave height was used to analyze solitary wave because of innate characteristics such as infinite wave length and period. The increase in SSC is dependent on the relative height of the solitary wave as shown in the linear regression curve for each wave breaking type in Fig. 8.

In most experiments the measurement of turbulence characteristics, such as turbulence intensity, was restrictive because of overestimation caused by disturbance of the channel or mechanical error generated from measuring equipment. Thus, to accurately generate turbulence intensity values, estimations from the numerical simulation were used to examine sediment transport along the slope. This was also done because the results of solitary wave height and velocity for each case have high accu-
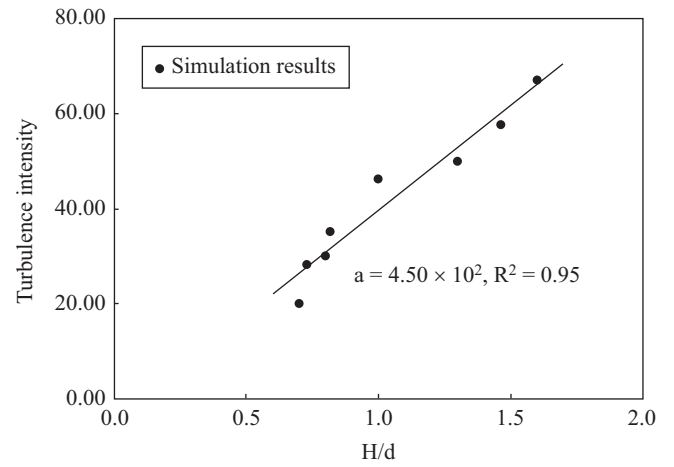
racy (< 5.0% discrepancy) between experiment and numerical simulation.

Turbulence intensity was are distributed in two distinct sections: one at spilling breaking type when H/d = 0.83 and the other at plunging breaking type when H/d = 0.87, (Fig. 8). In both experimental and numerical results, the run up/down velocities at Point 3, near the breaking point, were much higher than Point 2 in the transition zone. It can be deduced that the regression curve about the maximum turbulence intensity became increased with linear tendency in transition zone. For the spilling breaking type, SSC and turbulence intensity values were lower than in the plunging breaking type because of smaller vortices developed in the transition zone. Although there is an order-of-magnitude difference between the two breaking types, both still affected on the SSC values.

Incident wave characteristics were composed of run up velocity (V_s) on slope, wave period and height. During the regression analysis, a negative exponential curve is evident because the run up velocity increases with solitary wave height as presented in Eq. (4).

$$T1 = \begin{cases} -3.80\left(\dfrac{V_s H}{T}\right) & \textit{for Plunging breaking} \\[2mm] -9.25\times10^{-1}\left(\dfrac{V_s H}{T}\right) & \textit{for Spilling breaking} \end{cases} \quad (4)$$

Based on experimental results, turbulence intensity is presented as different equation in Eq. (4) for breaking wave types. From experimental and numerical results, it was observed that SSC was more strongly influenced by breaking wave condition than by run up velocity. The ranges of turbulence intensity are 12.56-35.41 for the spilling breaking wave type and 46.50-69.66 for the plunging breaking wave type, as shown in Fig. 10. The run-up velocity plays a significant role on SSC values in the spilling breaking wave type, with considerable disturbance of the sediment at the base caused by vortices in the plunging
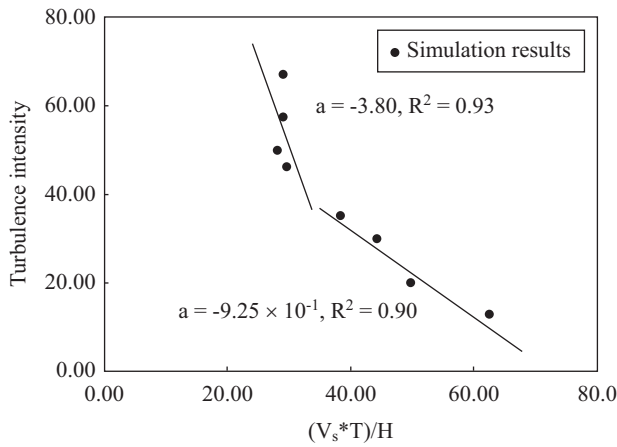
Journal of Marine Science and Technology, Vol. 25, No. 6 (2017)

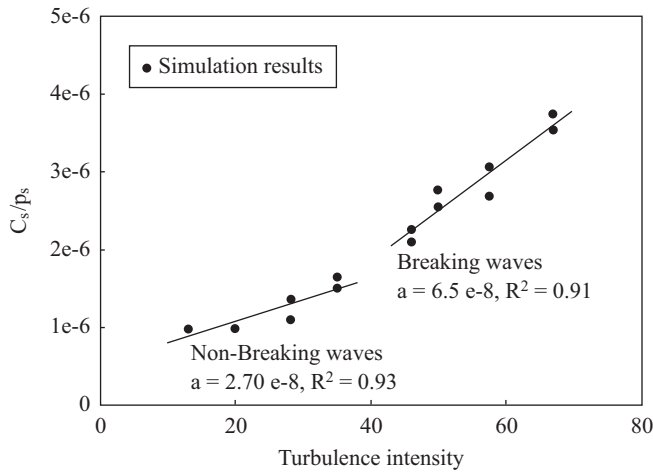**Fig. 10. Turbulence intensity curve against $(V_s{}^*T)/H$.**

Fig. 11. C_s/ρ_s curve against Turbulence intensity.

breaking wave type. This correlation is not evident when $(V_s{}^*T)/H = 28.6$ (Fig. 10).

For solitary wave height, velocity and period, SSC is presented using dimensional analysis with the non-dimensional parameter C_s/ρ_s that takes into account the effects of the disparity in specific gravity between the Joomoonjin sand and anthracite. Regression analysis of C_s/ρ_s versus turbulence intensity, shown in Fig. 11, indicates that there is a linear relationship between the two for each wave breaking type. For the plunging breaking wave type, there is a corresponding turbulence intensity of 46.50-69.66 and SSC values in the 1.91-3.04 g/m^3 range. Lower SSC values (0.98-1.21 g/m^3) are evident for the spilling breaking wave type. The regression curve gradient for the plunging breaking wave type is 5.24 times steeper than for the spilling breaking wave type, implying that the turbulence intensity of vortices in the former results in an increased suspended sediment load that is easily swept along a slope during wave run-up.

Based on both experimental and numerical results, the transport mechanism of suspended sediment near the bottom can be used to explain the impact of the plunging breaking wave on the sediment in the channel bed. Analysis about this phenomenon shows that turbulence intensity of vortices during wave breaking disturbs sediments near a channel bed, resulting in suspension of the sediments. Also, turbulence intensity in the 35.41 - 46.50 range is in the transition section between spilling and plunging breaking, which was not completely clear to define breaking wave type. It happened to rapidly increase SSC in this section, as shown in Fig. 11.

$$C_s/\rho_s = \begin{cases} 2.70\times10^{-8}\,T\cdot I & \text{for Plunging breaking} \\ 6.50\times10^{-8}\,T\cdot I & \text{for Spilling breaking} \end{cases} \qquad (5)$$

Eq. (5) is proposed from the regression analysis for each breaking wave type and can be used to estimate SSC for specific solitary wave conditions when the wave period, height and run-up velocity along the slope are known.

V. CONCLUSION

The suspended sediment concentrations (SSCs) carried by a solitary wave have been analyzed using both hydraulic experiments and numerical simulations. From experimental results, it was found that a solitary wave carried sediments in suspension, and that most amount of transport was occurred during wave run-up along the slope. Before the run-up, the disturbance of sediments near the bottom occurs because of turbulence that induces sediment instability. Numerical results show that the turbulence intensity during run-up contributes significantly to wave-sediment interactions and the transport of sediment in suspension. Thus, the passage of a solitary wave over and up a sandy slope results in erosion and deposition.

In addition, SSC was up to 3.43 times greater than during a plunging wave breaking than during a spilling wave breaking, which means it is highly dependent on the specific breaking type. Also, in terms of the turbulence intensity from numerical simulations, the SSC at plunging became 5.24 times higher than at spilling breaking, indicating that the change in the turbulence intensity that occurs when a wave breaks is the most major factor influencing suspended sediment transport.

Overall, this study provides the significant insight into the effects of the solitary wave height, the velocity of run up/down and turbulence intensity and these effects on the SSC occurred by a solitary wave. The relationship between SSC and wave characteristics has been quantified, allowing for estimate of SSC for several solitary wave conditions to be made, which can be used to examine SSC in field investigation and design procedures.

REFERENCES

Arthur, R. S. and O. B. Fringer (2014). The dynamics of breaking internal solitary waves on slopes. Journal of Fluid Mechanics 761, 360-398.

Carrier, G. F. and H. P. Greenspan (1958). Water waves of finite amplitude on a sloping beach. Journal of Fluid Mechanics 4(01), 97-109.

Chanson, H., S. I. Aoki and M. Maruyama (2002). An experimental study of tsunami runup on dry and wet horizontal coastlines. Science of Tsunami Hazards 20(5), 278-293.

Dohmen-Janssen, C. M., W. N. Hassan and J. S. Ribberink (2001). Mobile-bed effects in oscillatory sheet flow. Journal of Geophysical Research 106(C11), 27-103.

Flow Science, Inc. (2010) Flow-3D User Manual, Los Alamos, New Mexico.

Kobayashi, N. and A. R. Lawrence (2004). Cross-shore sediment transport under breaking solitary waves. Journal of Geophysical Research: Oceans 109(C3).

Moronkeji, A. and O. H. Rolla (2007, August). Physical modelling of tsunami induced sediment transport and scour. In Proceedings of the 2007 Earthquake Engineering Symposium for Young researchers, Seattle, Washington, USA (pp. 8-12).

Munk, W. H. (1949). The solitary wave theory and its application to surf problems. Annals of the New York Academy of Sciences 51(3), 376-424.

Pavanelli, D. and A. Pagliarani (2002). SW-Soil and Water: Monitoring Water Flow, Turbidity and Suspended Sediment Load, from an Apennine Catchment Basin, Italy. Biosystems Engineering 83(4), 463-468.

Smagorinsky, P. (1991). Expressions: Multiple Intelligences in the English Class. Theory & Research into Practice (TRIP). National Council of Teachers of English, 1111 Kenyon Rd., Urbana, IL 61801 (Stock No. 16647-0015, $7.95 members, $10.50 nonmembers).

Synolakis, C. E. (1987). The runup of solitary waves. Journal of Fluid Mechanics 185, 523-545.

Tsujimoto, G., T. Kakinoki and F. Yamada (2008, January). Time-space variation and spectral evolution of sandy beach profiles under tsunami and regular waves. In The Eighteenth International Offshore and Polar Engineering Conference. International Society of Offshore and Polar Engineers.

Zhao, Q., S. Armfield and K. Tanimoto (2004). Numerical simulation of breaking waves by a multi-scale turbulence model. Coastal Engineering 51(1), 53-80.